Taylor & Francis
Taylor & Francis Group

Vehicle System Dynamics
International Journal of Vehicle Mechanics and Mobility

ISSN: 0042-3114 (Print) 1744-5159 (Online) Journal homepage: http://www.tandfonline.com/loi/nvsd20

Performance of spade-less wheeled military vehicles with passive and semi-active suspensions during mortar firing

Ashkan Haji Hosseinloo , Nader Vahdati & Fook Fah Yap

To cite this article: Ashkan Haji Hosseinloo , Nader Vahdati & Fook Fah Yap (2012) Performance of spade-less wheeled military vehicles with passive and semi-active suspensions during mortar firing, Vehicle System Dynamics, 50:10, 1515-1537, DOI: 10.1080/00423114.2012.675076

To link to this article: http://dx.doi.org/10.1080/00423114.2012.675076

Vehicle System Dynamics
Vol. 50, No. 10, October 2012, 1515–1537

Taylor & Francis
Taylor & Francis Group

Performance of spade-less wheeled military vehicles with passive and semi-active suspensions during mortar firing

Ashkan Haji Hosseinloo[a], Nader Vahdati[b,*] and Fook Fah Yap[a]

[a]*School of Mechanical and Aerospace Engineering, Nanyang Technological University, 50 Nanyang Avenue, Singapore 639798, Singapore;* [b]*Department of Mechanical Engineering, The Petroleum Institute, PO Box 2533, Abu Dhabi, UAE*

(*Received 15 October 2011; final version received 4 March 2012*)

Many armies are replacing heavy slow tracked vehicles with their lighter wheeled counterparts for their high mobility and better shoot and scoot capabilities. These features make the vehicle hard to track and target in counter-battery fire. However, when firing high calibre guns, spades are needed to connect the vehicle chassis to the ground, so as to transmit parts of the large firing force directly to the ground. Use of spades hinders the vehicle mobility, while elimination of them paves the way for having quicker and more mobile wheeled vehicles. In this article, vibration response of a spade-less High Mobility Multi-purpose Wheeled Vehicle with a mounted mortar is studied and controlled using stock passive, optimised passive, and optimised semi-active dampers as primary suspensions. The spade-less vehicle with optimised passive and semi-active dampers has a better response in heave, pitch, and fore-aft motions and can fire with better accuracy compared to a spade-less vehicle with stock passive dampers. Simulation results indicate that the spades can be removed from wheeled military vehicles if the precautions are taken for the tyres.

Keywords: HMMWV; spade; MR damper; semi-active vibration control

1. Introduction

The success of wheeled military vehicles, such as Stryker, in different combat situations has prompted the US army to put its $40-billion ground combat vehicle procurement plan on hold to decide if it should invest on the next generation tracked vehicles or on the next generation wheeled vehicles [1]. Similar to the US army, many armies around the world are replacing heavy slow tracked vehicles with their lighter wheeled counterparts for their high mobility and better shoot and scoot capabilities, except for specific missions.

Tracked military vehicles, due to their greater weight and rigidity, can carry heavy artillery guns and mortars and fire them without a need for spades or outriggers. But the high weight of tracked vehicles has taken away speed and mobility.

*Corresponding author. Email: nvahdati@pi.ac.ae

ISSN 0042-3114 print/ISSN 1744-5159 online

http://dx.doi.org/10.1080/00423114.2012.675076
http://www.tandfonline.com

On the other hand, wheeled military vehicles are light weight, mobile, and require less energy and maintenance to run. However, due to their low weight, vehicle lift-off, flip over, slide, excessive chassis vibration, and tyre blowout are possible during mortar or artillery gun firing.

To prevent wheeled military vehicles from flipping over or bursting tyres during mortar firing, spades (or outriggers) are used to connect the vehicle to the ground, so as to transmit some of the mortar firing forces to the ground. Making use of spades contradicts with the essential philosophy of fast shoot and scoot. Addition of spades to wheeled military vehicles, during mortar fire, makes the vehicle stationary and hence a target for the enemy's fire. The spades also reduce the mobility of the vehicle, make the vehicle heavier, increase fuel consumption, and result in considerable time to plant into the ground and retract after firing.

However, if the spades can be eliminated, the wheeled vehicle will be mobile and never stationary, hence hard to track and target by the enemy. This idea is strengthened by the advent of new technologies in recoil systems with low-recoil force. One of the latest technologies is Super Rapid Advanced Mortar System (SRAMS) [2], with much lower recoil force in comparison to its counterparts. Therefore, research study is conducted in this article to see if spades can be eliminated by modelling a High Mobility Multi-Purpose Wheeled Vehicle (HMMWV) with a 120 mm gun (SRAMS) on it.

To this end, a multi-body dynamic model of a spade-less HMMWV with its mounted 120 mm SRAMS is developed and passive and semi-active shock absorbers are utilised as the primary suspension to control vehicle response during and after firing. The reason for considering semi-active dampers is that some of the wheeled military vehicles are already using semi-active dampers, such as magneto-rheological (MR) dampers, as their primary suspension system. Since these semi-active dampers are already there, the cost of implementation is reduced. Therefore, MR dampers could be used not only to control the vehicle chassis during manoeuvering, but also to control vehicle motion during mortar firing. M1078 and M1152 HMMWV are examples of the military vehicles that the US army awarded to the Lord Corporation for the evaluation and the installation of MR dampers as their primary suspensions [3,4]. The dynamic mathematical model of the HMMWV and SRAMS will be used to study the behaviour of the vehicle and its tyres during mortar firing with spades removed. The HMMWV mathematical model, control strategy, and simulation results will be discussed and presented in details in this article.

2. Literature review

Majority of the publications done on modelling, analysis and control of wheeled military vehicles are almost done only for manoeuvering purposes, rather than for integrated firing purposes. Only few studies have been carried out for analysis and control of recoil systems of the cannons, but not for cannons installed on the wheeled vehicles. In fact, it is very difficult to find many publications in this area since the military findings are usually kept confidential.

Many research studies have been conducted in the first category, i.e. modelling, analysis and control of the wheeled military vehicles over rough terrain. Sleight and Agrawal [5] and Ersal *et al.* [6] developed some reduced dynamic models for autonomous control and ride evaluation of a HMMWV. In addition, Grujicic *et al.* [7] modelled a HMMWV in the finite element modelling software ABAQUS/Explicit to investigate blast survivability and off-road performance of a HMMWV.

Control of these military vehicles for different manoeuvering criteria has been quite well studied mostly using semi-active skyhook, ground-hook, and hybrid control strategies to control semi-active primary suspensions. To this end, magneto-rheological dampers have

been commonly employed as the semi-active primary suspension systems. Gordaninejad and Kelso [8] employed Bingham plastic theory to model nonlinear behaviour of MR fluids to design a MR damper for the primary suspension of a HMMWV. Karakas *et al*. [9] experimentally investigated and compared the performance of a MR damper with that of an original equipment manufacturer damper as mounted in a quarter-car-test rig (representing a 1/4 car HMMWV) suspension. A year later, Liu *et al*. [10] did an experimental study on fuzzy logic control of a quarter-car-model of a HMMWV suspension system using a MR fluid damper and compared it with skyhook method. Although the studies conducted in the first category, normally manoeuverability and ride performance, did not take the integrated firing dynamics into account, reviewing their vehicle models and control strategies was useful for the integrated firing purposes and controls in this article.

Research studies conducted on the second category, i.e. analysis and control of recoil systems of mortars only, are also of very significant importance to the vibration control of the vehicles on which the mortars are mounted. A properly designed recoil system for a mortar can significantly reduce the transmitted force felt by the trunnion. Reducing this force enables employing larger calibre guns on military vehicles, which can handle higher impulse munitions. Higher impulse guns are necessary for defeating threats at greater distances while reduced transmitted force on trunnion pins allows for lighter vehicles which consequently results in greater mobility, deployability, and range. One of the mechanisms used to control recoil in recoil systems is fire out-of-battery (FOOB) mechanism. This mechanism, known also as soft recoil, can reduce the firing impulses by pre-accelerating (direction opposite of conventional recoil) the recoiling parts before ignition. Ahmadian and Poynor [11] studied MR dampers for controlling recoil dynamics. They showed that the recoil force increases and the recoil stroke decreases nonlinearly with an increase in the damping force. A year later, Ahmadian *et al*. [12] did an analytical study on FOOB recoil systems followed by their experimental work [13]. They concluded that when compared to conventional dampers, MR dampers can overcome firing faults of a FOOB system, namely pre-fire, hang-fire, and misfire, to a good extent. Hu *et al*. [14] tried to find an accurate nonlinear model for a recoil system equipped with MR dampers and studied its controllability under high impact loads.

Since the recoil cycle is very fast, usually about a few hundred milliseconds, the response time of the MR dampers becomes important and needs to be considered. Hu *et al*. [15] did a comprehensive study on the response evaluation of a MR gun recoil damper and its controllability under three control strategies, namely on-off, proportional-integral-derivative, and adaptive fuzzy control methods. Furthermore, Lijie *et al*. [16] did a similar investigation on modelling, adjustability and controllability of a MR gun recoil damper and tried to improve its response time and tracking ability by making use of different control strategies.

The objectives of the future combat system programme call for similar lethality to a current heavy tank but on an extremely lightweight vehicle of nominally 20 tonnes [17]. Prior experience with the M551 Sheridan, a light tank first put into production by the USA in 1966, raises concern that firing large calibre armaments from light vehicles may result in unacceptable crew discomfort and vehicular reaction during recoil [17]. But now, by the advent of the new technologies in military munitions and recoil systems, the trend towards lighter vehicles does not seem unachievable. FOOB, double recoil, the Davis gun, and active recoil mitigation suspension are a few of new integrated technologies being employed. One of the most recent recoil system technologies is SRAMS [2]. By employing special blast diffuser and newest technologies, the manufacturer claims to have the world's best mortar system with a recoil force of less than 14 tonnes when firing a 120 mm standard bomb at charge 9, directly measured from the pressure sensors mounted in the barrel [2]. This great achievement enlightens the possibility of mounting such mortars on light wheeled vehicles like HMMWVs, more than ever.

The authors could not find any published research on dynamic analysis and control of integrated mortar-wheeled vehicle systems. Moreover, there is an urgent need for more vehicle mobility and deployability in military technologies. Therefore, the authors decided to conduct a study to see if spades can be eliminated from light wheeled military vehicles such as a HMMWV, during mortar fire.

3. 2-D Heave/pitch/fore-aft spade-less vehicle model

3.1. *System modelling*

HMMWV is one of those popular military wheeled vehicles on which numerous mortars and artillery guns have been mounted. Figure 1 shows a typical HMMWV with a mounted SRAMS on it.

To study and control vehicle response during firing, a mathematical model representative of the integrated spade-less mortar-vehicle system has been developed. Since the vehicle-mortar system is considered to be symmetric, a two-dimensional (2-D) model is used rather than a three-dimensional one. The model as shown in Figure 2 consists of a five degrees-of-freedom vehicle model integrated with a one degree-of-freedom mortar system. The mortar system is rigidly pivoted and secured to the vehicle chassis through its platform; however, its elevation angle can be varied before firing to any desired value by its hydraulic system, but once the elevation angle α is chosen, the angle α between the chassis and the mortar, remains constant during mortar firing. Vehicle degrees-of-freedom are rear and front tyre vertical deflections, and chassis heave, pitch, and fore-aft motions, designated by $y_{tr}, y_{tf}, y_G, \theta$ and x, respectively. Recoil mass displacement relative to the barrel is designated by x_r. All other parameters used in Figure 2 are described in the nomenclature.

Since the mortar system is rigidly connected to the vehicle chassis and the elevation angle α once chosen, remains the same during firing, it is decided to combine the mortar and chassis masses and find the combined centre of gravity (cg) location, combined mass, and mass moment of inertia. For this purpose, a multi-body model of the mortar–chassis system is illustrated in Figure 3 and the equations relating these properties are derived in Section 3.2. All the parameters are defined in the nomenclature.

Figure 1. HMMWV with mounted SRAMS.

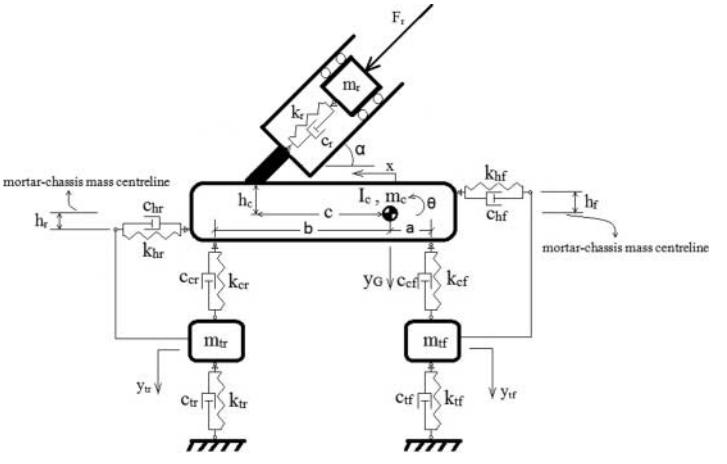

Figure 2. Schematic 2-D model of a HMMWV with mounted SRAMS.

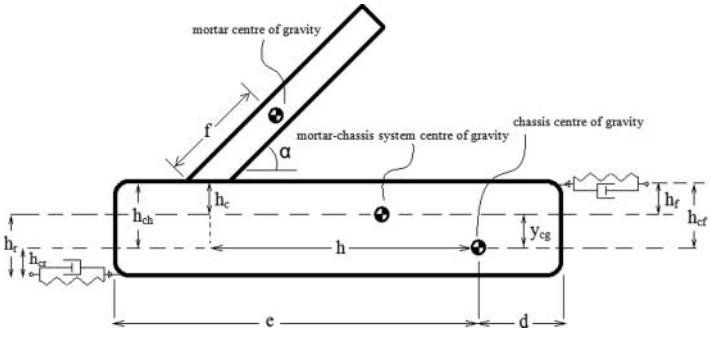

Figure 3. Multi-body mortar-chassis model.

3.2. *Combined mortar–chassis system parameters*

In this section, combined mortar–chassis system parameters (mass, mass moment of inertia, cg location, etc.) are derived using mortar and chassis parameters. From elementary physics and geometry shown in Figure 3, one can easily compute the combined system mass and its distances from rear and front tyres as shown below:

$$m_c = m_{ch} + m_{mor}, \tag{1}$$

$$b = \frac{m_{mor}[f\cos\alpha + (e-h)] + m_{ch}e}{(m_{mor} + m_{ch})}, \tag{2}$$

$$a = L - b. \tag{3}$$

Furthermore, combined system mass moment of inertia and vertical distances from its centre of gravity to mortar connection point, rear and front suspensions can be derived, respectively as follows:

$$I_c = I_{mor} + m_{mor}[(f\sin\alpha + h_c)^2 + (b - e + h - f\cos\alpha)^2] + I_{ch} + m_{ch}[(e-b)^2 + y_{cg}^2], \tag{4}$$

$$h_c = h_{ch} - y_{cg}, \tag{5}$$

$$h_r = h_{cr} + y_{cg}, \tag{6}$$

and,

$$h_f = h_{cf} - y_{cg}, \tag{7}$$

where y_{cg} is defined as:

$$y_{cg} = \left(\frac{m_{mor}}{m_{mor} + m_{ch}}\right)(f \sin\alpha + h_{ch}). \tag{8}$$

And finally, one can obtain the horizontal distance from the centre of gravity of the combined system to the mortar connection point as:

$$c = b - (e - h). \tag{9}$$

Now all the combined mortar-vehicle parameters are available from separate parameters of mortar and chassis. Using these parameters, equations of motion of the system are derived in Section 3.3.

3.3. *System dynamic equations*

Governing dynamic equations of motion for the model shown in Figure 2 can be derived by applying Newton's second law. In the derivation procedure, the pitch angle is assumed small and due to this assumption, some of the trigonometric functions can be linearised and simplified. After solving the system of equations, it will be seen that this assumption is acceptable. Direct application of Newton's second law for the chassis heave displacement will result in:

$$\begin{aligned}(k_r x_r + c_r \dot{x}_r)\sin\alpha + m_c g - k_{cr}(y_G + b\theta - y_{tr}) - c_{cr}(\dot{y}_G + b\dot{\theta} - \dot{y}_{tr})\\ - k_{cf}(y_G - a\theta - y_{tf}) - c_{cf}(\dot{y}_G - a\dot{\theta} - \dot{y}_{tf}) = m_c \ddot{y}_G.\end{aligned} \tag{10}$$

Equation of motion for the chassis pitch motion will be as follows:

$$\begin{aligned}&(k_r x_r + c_r \dot{x}_r)(c\sin\alpha + h_c\cos\alpha) + (k_{hr}x + c_{hr}\dot{x})(b\theta + h_r) - (k_{hf}x + c_{hf}\dot{x})(a\theta + h_f)\\ &- b[k_{cr}(y_G + b\theta - y_{tr}) + c_{cr}(\dot{y}_G + b\dot{\theta} - \dot{y}_{tr})] + a[k_{cf}(y_G - a\theta - y_{tf})\\ &+ c_{cf}(\dot{y}_G - a\dot{\theta} - \dot{y}_{tf})] = I_c\ddot{\theta}.\end{aligned} \tag{11}$$

Furthermore, Newton's second law for the chassis fore-aft motion leads to the following equation:

$$(k_r x_r + c_r \dot{x}_r)\cos\alpha - (k_{hr}x + c_{hr}\dot{x}) - (k_{hf}x + c_{hf}\dot{x}) = m_c\ddot{x}. \tag{12}$$

Governing equations for the rear and front tyre deflections are also found to be as follows, respectively:

$$m_{tr}g + k_{cr}(y_G + b\theta - y_{tr}) + c_{cr}(\dot{y}_G + b\dot{\theta} - \dot{y}_{tr}) - k_{tr}y_{tr} - c_{tr}\dot{y}_{tr} = m_{tr}\ddot{y}_{tr}, \tag{13}$$

and,

$$m_{tf}g + k_{cf}(y_G - a\theta - y_{tf}) + c_{cf}(\dot{y}_G - a\dot{\theta} - \dot{y}_{tf}) - k_{tf}y_{tf} - c_{tf}\dot{y}_{tf} = m_{tf}\ddot{y}_{tf}. \tag{14}$$

And finally, equation of motion for the recoil system will be as follows:

$$\begin{aligned} F_{\mathrm{r}} - k_{\mathrm{r}}x_{\mathrm{r}} - c_{\mathrm{r}}\dot{x}_{\mathrm{r}} + m_{\mathrm{r}}g\sin\alpha \\ &= m_{\mathrm{r}}[\mathbf{a}_{\mathrm{con}} + \mathbf{a}_{\mathrm{rel}} + \boldsymbol{\omega}\times(\boldsymbol{\omega}\times\mathbf{r}) + \boldsymbol{\alpha}\times\mathbf{r} + 2\boldsymbol{\omega}\times\mathbf{v}_{\mathrm{rel}}]_{\text{projection on } x_{\mathrm{r}} \text{ axis}} \\ &= m_{\mathrm{r}}[(\ddot{y}_{\mathrm{G}} + c\ddot{\theta} + h_{\mathrm{c}}\dot{\theta}^2)\hat{j} + (\ddot{x} + h_{\mathrm{c}}\ddot{\theta} - c\dot{\theta}^2)\hat{i} + \ddot{x}_{\mathrm{r}} + r\dot{\theta}^2]_{\text{projection on } x_{\mathrm{r}} \text{ axis}} \\ &= m_{\mathrm{r}}[(\ddot{y}_{\mathrm{G}} + c\ddot{\theta})\sin\alpha + (\ddot{x} + h_{\mathrm{c}}\ddot{\theta})\cos\alpha + \ddot{x}_{\mathrm{r}}]. \end{aligned} \tag{15}$$

In Equation (15), $\mathbf{a}_{\mathrm{con}}, \mathbf{a}_{\mathrm{rel}}, \boldsymbol{\alpha}, \boldsymbol{\omega}, \mathbf{v}_{\mathrm{rel}}$, and $\mathbf{r}$, are absolute acceleration vector of mortar connection point to the chassis, relative acceleration vector of the recoil mass in the coordinates attached to the mortar with the origin at its connection point, angular pitch acceleration vector, angular pitch velocity vector, relative velocity vector of the recoil mass in the aforementioned coordinates, and the displacement vector of the recoil mass in that coordinate system, respectively. Here, $\hat{i}$ and $\hat{j}$ are the fixed unit vectors in the direction of chassis fore-aft (horizontal) and heave (vertical) displacements.

3.4. *Nonlinear terms*

In Equation (11), there are four nonlinear terms resulting from the products $(k_{\mathrm{hr}}x + c_{\mathrm{hr}}\dot{x})(b\theta + h_{\mathrm{r}})$ and $(k_{\mathrm{hf}}x + c_{\mathrm{hf}}\dot{x})(a\theta + h_{\mathrm{f}})$. However, since the pitch angle is very small (refer to Figure 7), $a\theta$ and $b\theta$ will be much smaller than h_{f} and h_{r}, hence they can be neglected in the above two products.

In Equation (15), there are some more nonlinear terms, namely $c\dot{\theta}^2$, $h_{\mathrm{c}}\dot{\theta}^2$, and $r\dot{\theta}^2$. These terms are assumed small and thus negligible, and then their being negligible is proven by contradiction. To this, the equations of the motion are solved by the assumption that the nonlinearities are negligible. Then, the nonlinear acceleration term $c\dot{\theta}^2$ is plotted (Figure 5) along with the other linear acceleration terms in Equation (15), namely pitch, heave, and fore-aft accelerations. Finally, according to the plotted figure, it is shown that the nonlinear terms are negligible in comparison to the linear terms. If the assumption was not correct, the value of the nonlinear term should not have been found to be negligible, and thus, the assumption of them being negligible is correct by contradiction. Moreover, h_{c} and r are of the same order as c, and hence, $h_{\mathrm{c}}\dot{\theta}^2$ and $r\dot{\theta}^2$ are also assumed negligible.

3.5. *State space equations*

In order to have a compact form of equations and also for the ease of mathematical manipulation, equations of motion derived in Section 3.3 are rewritten in matrix form as below:

$$\mathbf{M}\ddot{\boldsymbol{z}} + \mathbf{C}\dot{\boldsymbol{z}} + \mathbf{K}\boldsymbol{z} = \boldsymbol{r}_{\mathbf{d}}, \tag{16}$$

where $\boldsymbol{z}$ is the displacement vector defined as:

$$\boldsymbol{z} = [y_{\mathrm{G}}\ \theta x\ y_{\mathrm{tr}}\ y_{\mathrm{tf}}\ x_{\mathrm{r}}]^{\mathrm{T}}. \tag{17}$$

In Equation (16), **M**, **K**, and **C** are mass, stiffness, and damping matrices, respectively, and are defined in Equations (18)–(20):

$$\mathbf{M} = \begin{bmatrix} m_c & 0 & 0 & 0 & 0 & 0 \\ 0 & I_c & 0 & 0 & 0 & 0 \\ 0 & 0 & m_c & 0 & 0 & 0 \\ 0 & 0 & 0 & m_{tr} & 0 & 0 \\ 0 & 0 & 0 & 0 & m_{tf} & 0 \\ m_r \sin\alpha & m_r c \sin\alpha + m_r h_c \cos\alpha & m_r \cos\alpha & 0 & 0 & m_r \end{bmatrix}_{6\times 6}, \tag{18}$$

$$\mathbf{K} = \begin{bmatrix} k_{cr}+k_{cf} & bk_{cr}-ak_{cf} & 0 & -k_{cr} & -k_{cf} & -k_r \sin\alpha \\ bk_{cr}-ak_{cf} & b^2k_{cr}+a^2k_{cf} & h_f k_{hf}-h_r k_{hr} & -bk_{cr} & ak_{cf} & -k_r(c\sin\alpha + h_c\cos\alpha) \\ 0 & 0 & k_{hf}+k_{hr} & 0 & 0 & -k_r\cos\alpha \\ -k_{cr} & -bk_{cr} & 0 & k_{cr}+k_{tr} & 0 & 0 \\ -k_{cf} & ak_{cf} & 0 & 0 & k_{cf}+k_{tf} & 0 \\ 0 & 0 & 0 & 0 & 0 & k_r \end{bmatrix}_{6\times 6}, \tag{19}$$

and,

$$\mathbf{C} = \begin{bmatrix} c_{cr}+c_{cf} & bc_{cr}-ac_{cf} & 0 & -c_{cr} & -c_{cf} & -c_r \sin\alpha \\ bc_{cr}-ac_{cf} & b^2c_{cr}+a^2c_{cf} & h_f c_{hf}-h_r c_{hr} & -bc_{cr} & ac_{cf} & -c_r(c\sin\alpha + h_c\cos\alpha) \\ 0 & 0 & c_{hf}+c_{hr} & 0 & 0 & -c_r\cos\alpha \\ -c_{cr} & -bc_{cr} & 0 & c_{cr}+c_{tr} & 0 & 0 \\ -c_{cf} & ac_{cf} & 0 & 0 & c_{cf}+c_{tf} & 0 \\ 0 & 0 & 0 & 0 & 0 & c_r \end{bmatrix}_{6\times 6}. \tag{20}$$

In Equation (16), $\boldsymbol{r_d}$ is the vector of body forces and firing force that can be written as below:

$$\boldsymbol{r_d} = [m_c g \;\; 0 \;\; 0 \;\; m_{tr} g \;\; m_{tf} g \;\; F_r + m_r g \sin\alpha]^T. \tag{21}$$

It is normally more convenient to transfer differential equations into state space format in order to reduce the order of differentiation. Equation (16) is a set of six scalar second-order differential equations which can be transformed to 12 first-order differential equations if transferred to the state space form. Thus, if Equation (16) is rewritten as:

$$\ddot{z} = -\mathbf{M^{-1}C}\dot{z} - \mathbf{M^{-1}K}z + \mathbf{M^{-1}}\boldsymbol{r_d}, \tag{22}$$

and state vector is set to:

$$\boldsymbol{x}_{12\times 1} = \begin{bmatrix} z^T & \dot{z}^T \end{bmatrix}^T \tag{23}$$

then, the state space equations will be as follows:

$$\dot{\boldsymbol{x}} = \mathbf{A}\boldsymbol{x} + \mathbf{R_d}. \tag{24}$$

In Equation (24), state matrix (**A**) and disturbance matrix ($\mathbf{R_d}$) are defined as below:

$$\mathbf{A}_{12\times 12} = \begin{bmatrix} 0_{6\times 6} & \mathbf{I}_{6\times 6} \\ -\mathbf{M}^{-1}\mathbf{K} & -\mathbf{M}^{-1}\mathbf{C} \end{bmatrix}, \tag{25}$$

$$\mathbf{R_d}_{12\times 1} = \begin{bmatrix} 0_{6\times 6} \\ \mathbf{M}^{-1} \end{bmatrix} \boldsymbol{r_d}. \tag{26}$$

The output will be the first six rows of the state vector (six degrees-of-freedom of the system) and their accelerations that can be calculated by making use of the state vector and Equation (22). In Section 4, the control strategy used to control the vehicle during firing will be discussed.

4. Primary suspensions

The function of a primary suspension system is to isolate the vehicle chassis from road disturbances, improve ride comfort, provide road holding and stability of the vehicle, and in this article, an additional requirement is needed which is to control chassis motion during mortar firing. In this article, three different primary suspension systems have been considered for the control of vehicle chassis during mortar fire and they are:

(1) Existing stock passive dampers
(2) Passive dampers optimised for firing
(3) Semi-active dampers optimised for firing

4.1. *Stock passive dampers*

Passive dampers, as the primary suspensions, are the most common and cheapest suspensions compared to semi-active and active suspensions. However, utilising passive dampers always lead to a compromise in road holding, handling and ride comfort of the vehicle. Since spades are used in most military vehicles, passive dampers are not optimised for mortar firing but only ride, and road handling and holding. With the removal of the spades, more compromise on the damping value of passive dampers need to be made in order to not only provide good ride, road holding and handling, but also mortar firing. The numerical value for existing stock dampers used for simulations in this study is given in Table 1.

4.2. *Passive dampers optimised for firing*

Since the current HMMWVs use spades to take the artillery gun reaction loads, the stock dampers are not optimised for artillery gun or mortar firing but for ride, road handling and holding. In our study, spades are removed; therefore, the passive dampers damping levels need to be optimised for mortar firing. To optimise the passive dampers for mortar firing, the dampers' damping coefficients are increased till the tyre forces reach their blowout threshold load. Thus, the obtained damping coefficient for a single damper in this study is $16,200\,\text{N.s.m}^{-1}$. This means an 80% increase in the already stiff stock dampers of the military vehicles which in turn significantly deteriorates the ride comfort of the vehicle. Despite this enormous increase in damping, the optimised passive dampers are investigated in this study with the hope of improving the body of the knowledge in this area and also for comparison with the optimised semi-active dampers.

Table 1. The vehicle parameters for the full-scale half-HMMWV model.

Parameter symbol	Value	Parameter symbol	Value
m_{ch}	1810 kg	c_{cf}	$9000\,\text{N.s.m}^{-1}$
m_{tr}	181 kg	c_{tr}	$4000\,\text{N.s.m}^{-1}$
m_{tf}	181 kg	c_{tf}	$4000\,\text{N.s.m}^{-1}$
I_{ch}	$2976\,\text{kg.m}^2$	L	3.3 m
k_{cr}	$163{,}300\,\text{N.m}^{-1}$	e	2 m
k_{cf}	$163{,}300\,\text{N.m}^{-1}$	h_{ch}	0.2 m
k_{tr}	$463{,}800\,\text{N.m}^{-1}$	h_{cf}	−0.2 m
k_{tf}	$463{,}800\,\text{N.m}^{-1}$	h_{cr}	0.2 m
c_{cr}	$9000\,\text{N.s.m}^{-1}$		

4.3. *Semi-active dampers optimised for firing*

Among different primary suspensions, active suspensions, utilising an actuator and sensors, have the best performance but they are very costly and not reliable compared to their passive and semi-active counterparts, thus not considered in this study. Semi-active dampers have most of the active suspension advantages while being low-cost and reliable. Moreover, most of the HMMWVs are being retrofitted with MR dampers, as their primary suspensions are normally operating in the semi-active mode. Therefore, semi-active dampers have been considered for this project.

To control the semi-active dampers, one of the most commonly used control policies is skyhook control which was first introduced in 1974 [18]. Skyhook damper is a fictitious damper that fixes the vehicle chassis to an inertial reference in the sky (Figure 4). The semi-active skyhook control policy is mathematically expressed as below,

$$c_{\mathrm{sa}} = \begin{cases} \dfrac{c_{\mathrm{sky}}\dot{y}}{(\dot{y}-\dot{y}_{\mathrm{b}})} c_{\mathrm{sky}}, & \dot{y}(\dot{y}-\dot{y}_{\mathrm{b}}) > 0 \\ c_{\mathrm{min}}, & \dot{y}(\dot{y}-\dot{y}_{\mathrm{b}}) \leq 0 \end{cases}, \tag{27}$$

where c_{sa} and c_{sky} are damping coefficients of semi-active damper and ideal skyhook damper, respectively. Here, c_{min} is the minimum semi-active damper damping coefficient, y and y_{b} are the mass and base displacements as shown in Figure 4 and $\dot{y}$ and $\dot{y}_{\mathrm{b}}$ are their time derivatives.

Semi-active skyhook control strategy is utilised in this article to suppress and control the vehicle motion during and after mortar firing. The continuous skyhook control is applied to both rear and front suspensions and the results are presented in Section 5. The semi-active dampers are optimised with the same method as the passive dampers are optimised with. The optimised semi-active dampers have skyhook damping coefficient equal to $11,000\,\mathrm{N.s.m^{-1}}$.

Stiffness and damping of the vehicle in the horizontal direction have two components; one is constant and resulting from the rubber bushings and other constant sources and the other part is the horizontal portion of the vertical stiffness and damping resulting from deviation of the suspension from its vertical position. The latter part is inherently variable and dependent on the deviation angle of the vertical suspension spring and damper, but for simplicity and avoiding nonlinearity, it is assumed to be a constant percentage of the vertical suspension (it will be further addressed in Section 5.1). Therefore, this part of the horizontal damping will be also subjected to the skyhook control as it is inherently a percentage of the suspension dampers.

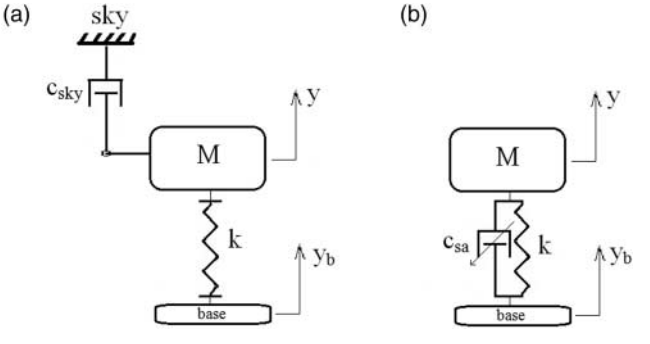

Figure 4. Schematic figure of: (a) ideal skyhook and (b) semi-active skyhook configurations.

4.4. *Method of simulation*

In this article, the intention is to monitor and control the dynamic response of the HMMWV chassis motion to mortar firing without spades. The spade-less vehicle response is going to be monitored and analysed to see if any of the probable problems would occur. The probable problems include excessive chassis vibration, firing inaccuracy, tyre blowout, vehicle slide, vehicle lift-off, large suspension travel, and hydraulic lock-up. Then, it is examined to see if these problems can be prevented by the effective use of primary suspensions or by taking other design precautions.

Furthermore, in simulation results, the static displacement of all masses has been subtracted from all the displacement figures; therefore, all plots begin from zero displacement.

5. Simulation results

5.1. *Vehicle description and properties*

As mentioned earlier in Section 3, a five degrees-of-freedom mathematical model is considered for the HMMWV vehicle. The geometric and physical properties of the vehicle chassis are used from those provided by Aardema [19] for a standard HMMWV without any shelter or mortar. Vehicle suspension and tyre properties are adopted from [9], and are tabulated in Table 1. All the parameters in the table are introduced in the nomenclature.

Horizontal stiffness and damping have two components as discussed in Section 4.3. The first part which is resulting from bushings and other constant sources are assumed to be 7% of their corresponding passive vertical stiffness and damping. The other component of horizontal stiffness and damping which is due to the deviation of vertical suspension from vertical position is assumed to be equal to 15% of their corresponding vertical values [20]. In Equation (27), the damping coefficient of ideal skyhook dampers (c_{sky}) is set to 11,000 N.s.m^{-1}, minimum semi-active damping coefficient (c_{min}) is idealised to be 0 and the semi-active skyhook damping coefficients of the suspension dampers are generally variable (continuously varying). During the simulation studies, it was seen that as the skyhook or passive damping is increased, there is a conflicting trend between the tyre blowout and the other probable problems in the vehicle such as vehicle slide and inaccuracy. That is, as the skyhook damping increases, the tyres' forces increase, making them more likely to blowout while the other problems such as vehicle slide, lift-off, excessive vibration, and firing inaccuracy are mitigated. In other words, the tyre force is a stopping limit for the semi-active dampers. Therefore, the skyhook damping is increased as much as the tyres' forces will not exceed the maximum capacity of a particular E-range tyre, i.e. 22 kN, and thus is optimised. The optimised skyhook damping is 11,000 N.s.m^{-1} as stated earlier. Moreover, the friction coefficient between tyres and the ground is assumed to be 0.7 [21].

5.2. *Mortar system description and properties*

The mortar system considered in this article is a 120 mm smoothbore SRAMS. The unique design of SRAMS, coupled with other features of its recoil mechanism, has led the SRAMS to achieve an extremely low recoil reading of 13.6 tonnes when firing a 120 mm standard bomb at charge 9 [2]. The recoil firing force is modelled as a half-sine force with a total duration of 50 ms and an amplitude of 135.7 kN. The barrel elevation angle is assumed to be 40° in the simulations unless otherwise specified. Other properties of the mortar are presented in Table 2.

Table 2. The mortar parameters for the full-scale SRAMS model.

Parameter symbol	Value	Parameter symbol	Value
m_r	400 kg	k_r	80,345 N.m^{-1}
m_{mor}	800 kg	h	0.75 m
I_{mor}	2000 kg.m^2	f	1 m

The recoil system of a gun is essentially a critically damped system to absorb the recoil force [22]. Therefore, the recoil damping is set to a value, so that the local recoil damping ratio is equal to unity. One should note that the properties given here for the mortar system are for a full-scale full mortar model, but the properties given for the vehicle are for a full-scale half-car model. Therefore, once substituting them into the system equations, one should either multiply the vehicle properties by 2 or the mortar properties by 0.5. The geometric properties will not change for this matter. Then, with all the vehicle and mortar system properties and specifications along with the equations derived in Section 3 and utilising the semi-active control strategy described in Section 4, the simulations are carried out in MATLAB Software and the results are presented in Sections 5.3 and 5.4.

5.3. *Nonlinear terms*

In Section 3.4, it was mentioned that the nonlinear terms $c\dot{\theta}^2$, $h_c\dot{\theta}^2$, and $r\dot{\theta}^2$ were negligible in comparison to the other terms in Equation (15) and thus, were neglected. Figure 5 illustrates and compares time histories of heave, pitch, and fore-aft accelerations with that of square pitch velocity of the vehicle with stock passive suspension. Since the coefficients of these terms in Equation (15) are of the same order, accelerations are plotted in this figure without multiplication by their coefficients in the equation. As can be seen from Figure 5, the order of square pitch velocity is considerably smaller than that of other accelerations appeared in Equation (15). Quantitatively speaking, expected values of heave, pitch, and fore-aft accelerations are, respectively, 266, 100, and 420 times greater than that of square pitch velocity. Therefore, it was a reasonable assumption to neglect the nonlinear terms.

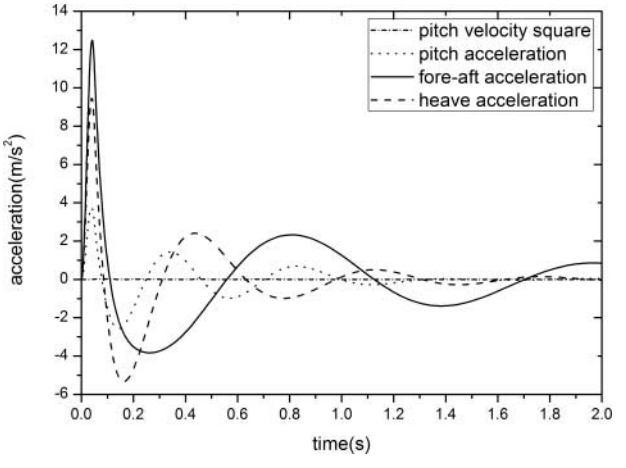

Figure 5. Comparison of order of square pitch velocity with heave, pitch, and fore-aft accelerations of the vehicle with stock passive suspension.

5.4. *Results*

When the spade is removed from a wheeled military vehicle during mortar firing, the vehicle chassis heave, pitch, and fore-aft motions will increase and the firing accuracy of the mortar system will be affected. With no spade, it is possible that the vehicle may slide or lift-off the ground or possibly flip over during mortar firing. To study the behaviour of the vehicle without the spade with different suspension systems (stock passive dampers, versus optimised passive dampers, versus optimised semi-active dampers, versus ideal skyhook dampers) during mortar firing, the following parameters are plotted:

(1) Chassis heave, pitch, and fore-aft motions
(2) Front and rear suspension travels
(3) Forces experienced by the front and rear tyres
(4) Horizontal forces exerted on the tyres

Here, in this section, a brief description of each figure is first given and towards the section end, two tables are used to summarise the simulation findings. All the simulations were run for 5 seconds and all the displacement figures are plotted from the static equilibrium position.

5.4.1. *Chassis heave, pitch, and fore-aft motions*

The removal of the spades from the vehicle might cause extreme vibrations in the heave, pitch, and fore-aft motions during mortar firing. This can bring about problems both for the vehicle and the crew. Heave, pitch, and fore-aft displacements of the HMMWV for stock passive, optimised passive, optimised semi-active skyhook, and ideal skyhook dampers are compared in Figures 6–8. According to Figures 6–8, the chassis heave, pitch, and fore-aft motions of the vehicle with optimised semi-active suspension have been improved compared to the vehicle with stock and optimised passive suspension systems.

For fore-aft vibration of the vehicle, the optimised semi-active control has the best performance in terms of both amplitude and range, even better than the ideal skyhook. In the semi-active skyhook control, damping coefficients of the semi-active dampers can go higher than that of the ideal skyhook dampers to achieve a closer performance of the ideal skyhook, and since a percentage of this vertical damping will contribute to the horizontal damping of

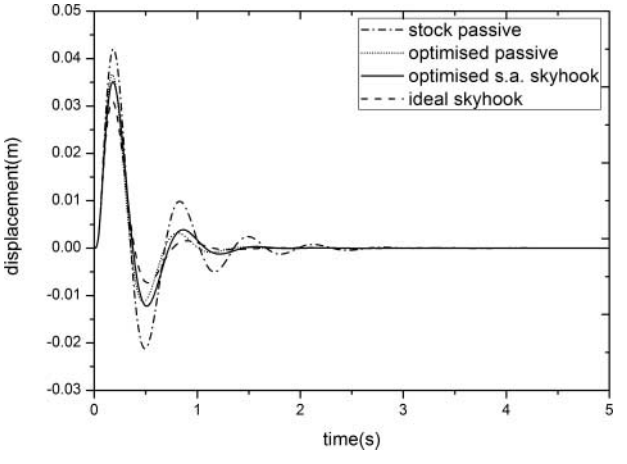

Figure 6. Time history of vehicle heave with stock passive, optimised passive, optimised semi-active skyhook, and ideal skyhook suspensions.

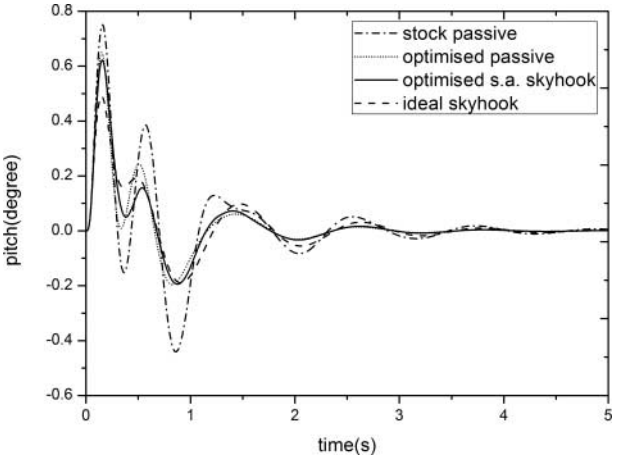

Figure 7. Time history of vehicle pitch with stock passive, optimised passive, optimised semi-active skyhook, and ideal skyhook suspensions.

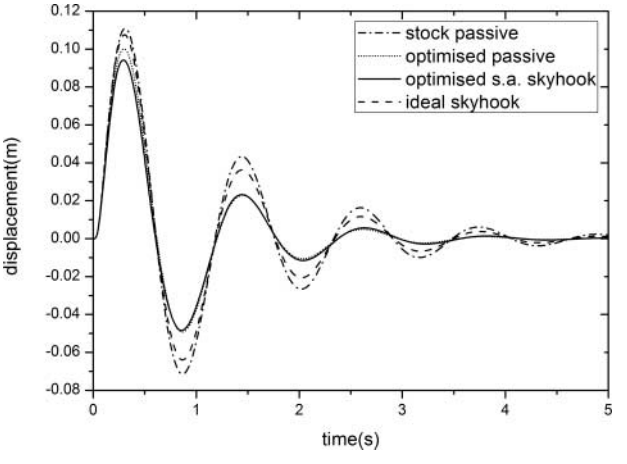

Figure 8. Time history of vehicle fore-aft motion with stock passive, optimised passive, optimised semi-active skyhook, and ideal skyhook suspensions.

the chassis, the high damping coefficients dampen horizontal motion of the vehicle even faster than the ideal skyhook.

5.4.2. *Firing accuracy*

The chassis pitch angle affects the firing accuracy. If the momentum velocity of the bomb, leaving the barrel, is designated by $\boldsymbol{V}_0$, the firing range will be,

$$R = \frac{(V_0^2 \sin 2\alpha)}{g}, \tag{28}$$

where R is the range, α is the elevation angle of the mortar from the horizontal plane, and g is gravitational acceleration. By assuming a half-sine firing force as mentioned before, the

impulse imparted to the bomb will be,

$$\int_0^T F_{\text{firing}} \mathrm{d}t = \int_0^T F_{\text{r}} \sin\left(\frac{\pi t}{T}\right) \mathrm{d}t = \frac{2F_{\text{r}}T}{\pi}, \tag{29}$$

where F_{firing} and F_{r} are firing and recoil forces, respectively, and T is the firing duration that is 50 ms. Therefore, if the bomb mass is designated by m, the bomb velocity leaving the barrel, i.e. $\boldsymbol{V}_{\text{o}}$ will be,

$$V_{\text{o}} = \frac{2F_{\text{r}}T}{m\pi}. \tag{30}$$

Now, one can evaluate the change in the range in terms of a change in the elevation angle by differentiating Equation (28) with respect to α. Differentiating Equation (28) and substituting $\boldsymbol{V}_{\text{o}}$ from Equation (30) yields,

$$\mathrm{d}R = \frac{2}{g}\left(\frac{2F_{\text{r}}T}{m\pi}\right)^2 \cos(2\alpha)\mathrm{d}\alpha. \tag{31}$$

If the bomb mass is assumed to be 15 kg and the elevation angle to be $\pi/4.5$ radians (40°), using Equation (31), the firing inaccuracy will be improved by 5.2 m and 6.7 m if the stock passive suspension is replaced by optimised passive and semi-active suspensions, respectively. Effectiveness of the optimised passive and semi-active suspensions in firing accuracy becomes even more evident if the firing takes place at other elevation angles. For example, if the firing elevation angle increases to $\pi/3$ radians (60°), firing inaccuracy will be improved by 17.6 m and 23.6 m in optimised passive and semi-active suspensions, respectively.

5.4.3. *Tyre blowout and vehicle lift-off*

Outriggers (or spades) are used to prevent tyre blowout during mortar firing, but if spades are removed, tyres are more likely to blowout due to the sever shock and excessive load transmitted to them. Tyres bursting point is usually characterised by a maximum deflection, a maximum pressure, or a maximum load. In this study, rear and front tyre loads are monitored and their time histories are plotted in Figures 9 and 10.

As compared to the stock passive suspension, the optimised semi-active suspension has smaller front tyre forces and slightly larger rear tyre forces, while the optimised passive

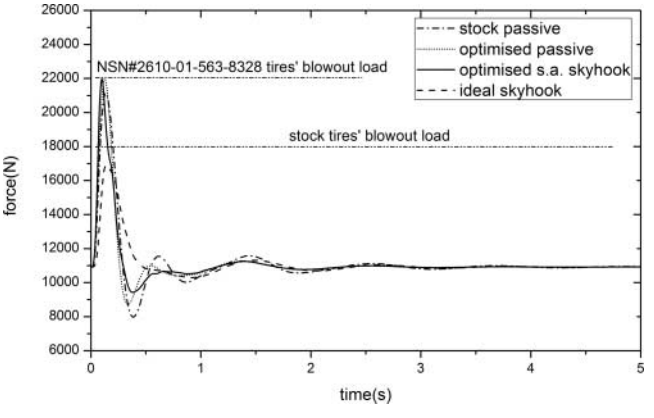

Figure 9. Time history of rear tyre force with stock passive, optimised passive, optimised semi-active skyhook, and ideal skyhook suspensions.

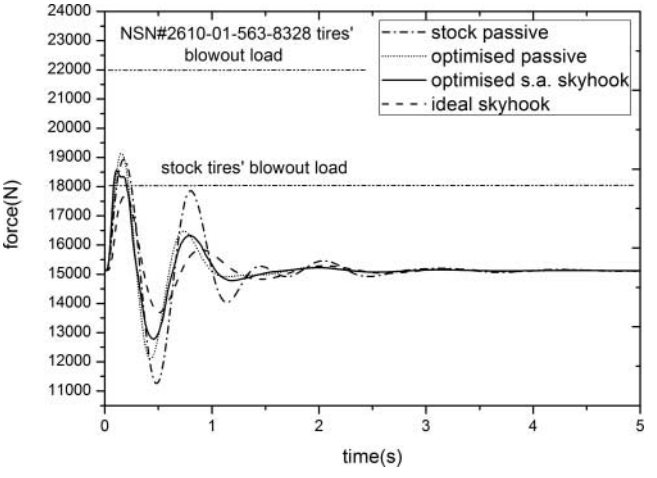

Figure 10. Time history of front tyre force with stock passive, optimised passive, optimised semi-active skyhook, and ideal skyhook suspensions.

suspension has larger tyre forces for both rear and front tyres. The maximum forces experienced by the rear and front tyres are about 22 kN and 19 kN for the vehicle with optimised passive suspensions and 22 kN and 18.5 kN for the vehicle with optimised semi-active suspensions. The tyres commonly used in HMMWVs can resist up to 18 kN. Thus, the current tyres used in HMMWVs will blowout if the spades are removed.

However, by a thorough search in the internet, the authors found other ruggedised tyres for HMMWVs capable of handling the maximum tyre forces occurring in the semi-actively controlled dampers. Baja T/A off-road tyres of BF Goodrich company with NSN number of 2610-01-563-8328 are examples of E-range high capacity tyres capable of handling more than 22 kN load when stationary. Furthermore, there is a new generation of airless tyres called Tweel, first commercialised by Michelin. These airless tyres have higher load capacity than their pneumatic counterparts due to the airless characteristics. To design even higher capacity tyres for military applications, particularly for HMMWVs, Resilient Technologies and Wisconsin-Madison's Polymer Engineering Center are currently developing a patent-pending non-pneumatic tyre that can even survive an improvised explosive device attack, and still make a 50 mph getaway [23]. Said tyre is fundamentally a round honeycomb wrapped in thick black tread. The latter airless tyre, to be released by the end of 2011, is currently being tested on a Wausau-based National Guard HMMWV. Another effort to mitigate the risk of tyre blowout is the modification of the pressure of the tyres. Nowadays, the technology on some of luxury passenger vehicles allows the driver to decrease or increase the tyre pressure remotely from inside the car. If this technology is installed on a HMMWV, the pressure can be changed accordingly when firing. Consequently, since the load capacity of tyres significantly depends on their pressure, this method can increase the tyre's load capacity and, hence prevent the tyre blowout.

Another concern during mortar firing without a spade is vehicle lift-off which is not desirable and can impact firing accuracy. The vehicle lift-off can be tracked in terms of tyre forces. If they go into negative values (expansion of tyres), it means that the tyres have lifted off the ground. The tyre forces shown in Figures 9 and 10 are total forces including their initial values due to the vehicle weight, therefore; they can be used to check if the tyres have lifted off. As shown in these figures, the tyre forces are well above zero, so no lift-off occurs for any of the suspensions.

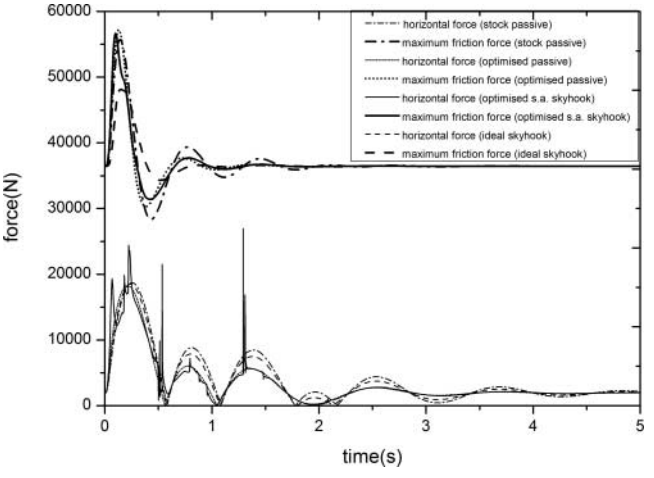

Figure 11. Time history of total horizontal and friction forces exerted on the tyres through the suspension and the ground in stock passive, optimised passive, optimised semi-active skyhook, and ideal skyhook suspensions.

5.4.4. *Vehicle slide*

Because of the horizontal component of the firing force, the vehicle could slide on the ground horizontally. If the horizontal force exerted on the tyres is greater than the maximum opposing static friction force (each tyre normal force times friction coefficient), the vehicle will slide. Figure 11 shows the horizontal force exerted on the tyres through the suspension and the static friction force experienced by the tyres.

As shown in Figure 11, no horizontal force curve intersects its corresponding friction force curve in any of the four suspensions. This means no sliding occurs for any of the stock passive, optimised passive, optimised semi-active skyhook, and ideal skyhook suspensions.

5.4.5. *Suspension travel*

If the dampers bottom out too many times during mortar firing, the dampers will eventually cease to function. To see if the dampers bottom out, suspension travel (or rattle space) of the rear and front suspensions of the vehicle is plotted in Figures 12 and 13. Suspension travel is the total up and down movement of the suspension with the axle on a level plane. If the suspension travel is larger than the maximum allowed value, the dampers will bottom out. According to Figure 12, the suspension travel for the rear suspension is 5.3, 3.8, 4.2, and 3.2 cm for stock passive, optimised passive, optimised semi-active skyhook, and ideal skyhook suspensions. Furthermore, according to Figure 13, the suspension travel for the front suspension is 4.4, 1.7, 2.5, and 2.1 cm for stock passive, optimised passive, optimised semi-active skyhook, and ideal skyhook suspensions. The suspension travels for both rear and front suspensions are in acceptable range, meaning that the dampers will not bottom out.

5.4.6. *Other practical issues*

The maximum values of the suspension damping forces should be in a feasible range. Figures 14 and 15 show time histories of the rear and front suspension damping forces for the stock passive, optimised passive, optimised semi-active skyhook, and ideal skyhook dampers. The maximum damping forces for a single damper of the rear and front suspensions in the

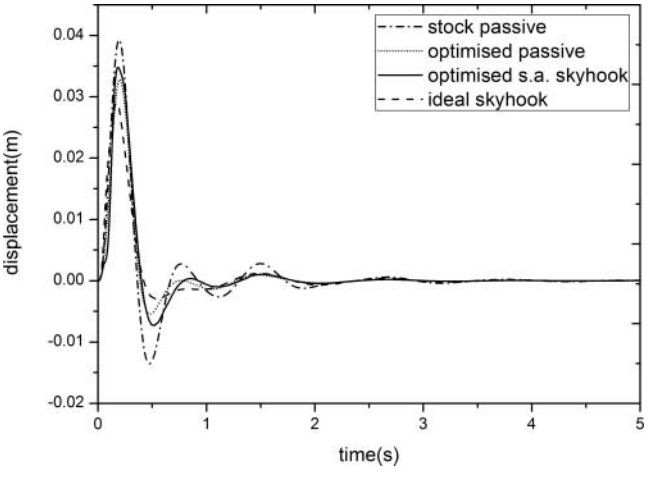

Figure 12. Time history of rear suspension travel for stock passive, optimised passive, optimised semi-active skyhook, and ideal skyhook suspensions.

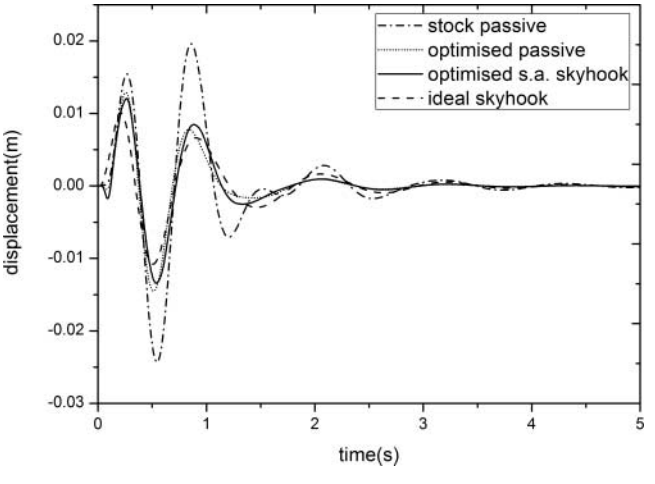

Figure 13. Time history of front suspension travel for stock passive, optimised passive, optimised semi-active skyhook, and ideal skyhook suspensions.

semi-active suspension are about 6600 N and 2100 N, respectively. These damping forces are achievable by a properly designed semi-active damper. If MR dampers are to be used as the semi-active dampers, the above-mentioned damping forces are easily achievable.

Another practical issue to consider is the response time of the semi-active dampers. Semi-active dampers can be used in the recoil system of the mortar system or in the primary suspension. There is significant advantage for using them in the suspension system rather than the recoil system, particularly if the semi-active dampers are MR-based. While the response time of the MR fluid is of the order of milliseconds, the overall response time of the electronic and magnetic circuits and the control system can be much longer (50–100 ms). Since the overall response time of MR dampers can be greater than, 50 ms mortar firing pulse, utilising the MR dampers in the recoil system will not be efficient.

In this article, it was observed that the force pulse duration has increased by 500% after transmission through the recoil suspension system. This enables the semi-active dampers

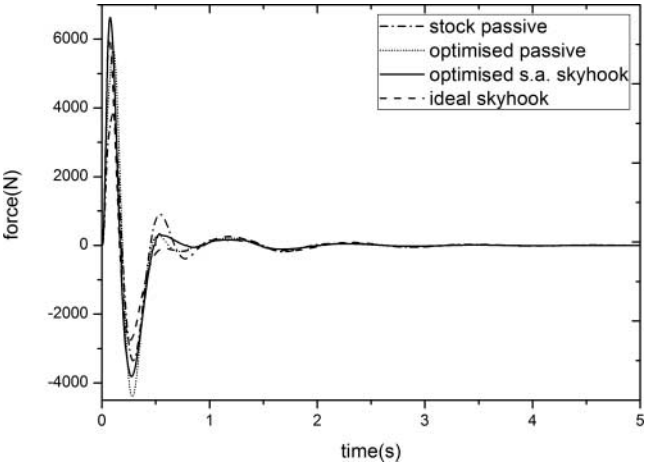

Figure 14. Time history of rear suspension damping force for a single damper in stock passive, optimised passive, optimised semi-active skyhook, and ideal skyhook suspensions.

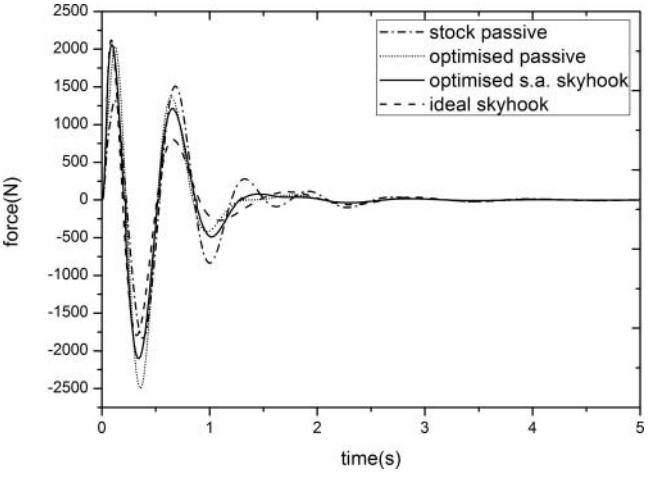

Figure 15. Time history of front suspension damping force for a single damper in stock passive, optimised passive, optimised semi-active skyhook, and ideal skyhook suspensions.

and the control system to have sufficient time to react and respond to the firing excitation, and consequently, they will have better performance than semi-active dampers (particularly MR-based dampers) used in the recoil suspensions.

Orifices used in most shock absorbers, to create damping, are small in diameter and if the working fluid is forced to pass through them at high velocities, flow resistance gets very high therefore, pressure rises, and the shock absorbers burst. This can occur if the damper is subjected to high input velocities or forces. In military applications, where high shock and firing forces are imparted to the system in a very short period of time, the lock-up phenomenon of the dampers are very likely to arise. Therefore, the dampers should be especially designed to prevent any hydraulic lock-up occurring. One should note that if the dampers are used in the recoil system, this issue becomes even more serious and probable, since the dampers will be subjected to higher forces in a shorter period of time compared to the case when they are mounted in the primary suspension system.

Table 3. Percentage reduction in amplitude, range, and settling time.

		Amplitude (%)	Range (%)	Settling time (%)
Heave	Stock passive	0	0	0
	Optimised passive	13	24	38
	Optimised semi-active skyhook	17	25	30
	Ideal skyhook	26	40	45
Pitch	Stock passive	0	0	0
	Optimised passive	13	29	42
	Optimised semi-active skyhook	17	32	30
	Ideal skyhook	35	43	14
Fore-aft	Stock passive	0	0	0
	Optimised passive	10	18	34
	Optimised semi-active skyhook	15	22	32
	Ideal skyhook	3	6	20
Rear suspension travel	Stock passive	0	0	0
	Optimised passive	16	28	21
	Optimised semi-active skyhook	11	20	19
	Ideal skyhook	26	39	−6
Front suspension travel	Stock passive	0	0	0
	Optimised passive	34	38	28
	Optimised semi-active skyhook	38	42	26
	Ideal skyhook	48	52	−3

Table 4. Tyre blowout, vehicle lift-off and slide occurrences, and firing accuracy.

	Stock passive	Optimised passive	Optimised semi-active skyhook	Ideal skyhook
Tyre blowout	Yes	Yes	Yes	Yes
Vehicle lift-off	No	No	No	No
Vehicle slide	No	No	No	No
Firing accuracy	Worst	Second better	First better	Best

5.4.7. *Results in tabular form*

In Table 3, the reductions in different response parameters (heave, pitch, etc.) in different suspensions in terms of amplitude, range (maximum to minimum) and settling time are given in percentage. The settling time error tolerance in this article is set to 2%. The reduction is calculated relative to the stock passive suspensions, and that is why the stock passive rows are all 0. The occurrence of tyre blowout, vehicle lift-off, and vehicle slide is tabulated in Table 4 for the four suspensions and their firing accuracies are compared.

6. Summary and conclusion

Since no similar study as given in this article was found in literature, the authors embarked upon conducting a study to see what effects, the removal of spades from wheeled military vehicles during mortar firing, will have on the vehicle response and mortar firing accuracy. With the removal of spades, the vehicle becomes more mobile and difficult to be spotted by the enemy, but the removal of the spades can possibly result in excessive chassis vibration, firing inaccuracy, tyre blowout, vehicle slide, vehicle lift-off, large suspension travel, and hydraulic lock-up of the shock absorbers. To study the effect of spade removal, a spade-less pitch-heave dynamic model of a HMMWV with a 120 mm mortar was developed. Three primary suspension systems, namely stock passive dampers, optimised passive dampers, and optimised semi-active dampers with the semi-active skyhook control were compared in terms of vehicle

response and firing accuracy and the results were compared with the same HMMWV attached to ideal skyhook passive dampers.

The simulation results show that the semi-active suspensions provide better performance than the stock and optimised passive suspensions, in terms of vehicle vibration response such as heave, pitch, fore-aft motions, and firing accuracy. When it comes to mortar firing accuracy, stock passive dampers are not recommended. No vehicle slide or lift-off, in either the stock and optimised passive or semi-active suspensions, was observed.

Simulation results show that the required semi-active damper damping forces to control chassis motion during firing are in feasible range. Suspension travel of the semi-active dampers was also monitored and there was no excessive suspension travel that could lead to dampers bottoming out. Furthermore, the hydraulic lock-up issues of the dampers can be easily prevented by a proper design of the dampers.

Simulation results indicate that if spades are removed from the existing HMMWVs with stock tyres, the tyres will burst during mortar firing. However, the authors found other ruggedised tyres capable of handling the maximum tyre forces occurring in the semi-actively controlled dampers such as Baja T/A off-road tyres of BF Goodrich company with NSN number of 2610-01-563-8328. Therefore, the problem of tyre blowout in the case of spade removal can be prevented by choosing appropriate, stronger, and more ruggedised tyres.

One should note that by increasing the passive suspension damping coefficients, similar results as those for the semi-active suspension can be achieved during mortar firing as shown in Figures 6–15. But the problem with increase in passive dampers damping coefficients is that they cannot be decreased when vehicle is no longer firing and is being driven on rough terrain. In this case, large damping in the suspension results in poor ride and comfort quality of the vehicle. If a two mode passive damper can be designed to provide different damping levels, one value during mortar firing, and another value during normal driving conditions, then semi-active dampers will not be needed. As indicated previously in this article, since many armies around the world are already considering MR-dampers as the primary suspension in their military vehicles (e.g. such as HMMWV and Stryker), we recommend MR-dampers as the choice of primary suspension since they provide not only ride comfort and road holding, but also can provide chassis motion control during mortar firing. Simulation results indicate that the spade removal from HMMW is possible and feasible if ruggedised tyres are used. This achievement consequently, reduces the vehicle weight and the time duration for shoot and scoot, thus, results in more mobility for the HMMWV.

Acknowledgements

The authors gratefully acknowledge the financial support of Singapore Technologies Kinetics (ST Kinetics).

References

[1] M. Fabey (15 October 2010), GCV may decide fate of army tracked vehicles. *Aviation Week* [Magazine]. Available at http://www.aviationweek.com/aw/generic/story_channel.jsp?channel=defense&id=news/dti/2201/10/01/DT_10_01_2010_p42-254759.xml&headline=GCV%20May%20Decide%20Fate%20Of%20Army%20Tracked%20Vehicles.

[2] C.F. Foss, *Singapore Technologies Kinetics Mounts Mortar System on HMMWV*, *Jane's Defence Weekly*, March 2005.

[3] K. Kayler, *LORD corporation awarded contract for evaluation of MR suspension system on HMMWV*, (2009). Available at http://www.lord.com/news-center/press-releases/lord-corporation-awarded-contract-for-evaluation-of-mr-suspension-system-on-hmmwv.xml.

[4] K. Kayler, *LORD corporation awarded contract for MR suspension installation and test on US Army LMTV*, (2010). Available at http://www.lord.com/news-center/press-releases/lord-corporation-awarded-contract-for-mr-suspension-installation-and-test-on-us-army-lmtv.xml.

[5] R. Sleight and S.K. Agrawal, *Dynamic model of a four-wheel-drive HMMWV*, ASME Design Engineering Technical Conferences and Computers and Information in Engineering Conference, Salt Lake City, UT, USA, 2004.
[6] T. Ersal, B. Kittirungsi, H.K. Fathy, and J.L. Stein, *Model reduction in vehicle dynamics using importance analysis*, Veh. Syst. Dyn., 47 (2009), pp. 851–865.
[7] M. Grujicic, G. Arakere, H. Nallagatla, W. Bell, and I. Haque, *Computational investigation of blast survivability and off-road performance of an up-armoured high-mobility multi-purpose wheeled vehicle*, Proc. Inst. Mech. Eng., Part D: J. Automob. Eng., 223 (2009), pp. 301–325.
[8] F. Gordaninejad and S.P. Kelso, *Magneto-Rheological Fluid Shock Absorbers for HMMWV*, Proceedings of SPIE Conference on Smart Structures and Materials – Damping and Isolation, San Diego, CA, 2000.
[9] E.S. Karakas, F. Gordaninejad, C.A. Evrensel, M.-S. Yeo, Y. Liu, and H. Sahin, *Control of a Quarter HMMWV Suspension System using a Magneto-Rheological Fluid Damper*, Proceedings of SPIE Conference on Smart Structures and Materials – Damping and Isolation, San Diego, CA, 2004.
[10] Y. Liu, F. Gordaninejad, C.A. Evrensel, E. Sinan Karakas, and U. Dogruer, *Experimental Study on Fuzzy Control of a HMMWV Suspension System using Magneto-Rheological Fluid Damper*, Proceedings of SPIE Conference on Smart Structures and Materials – Smart Structures and Integrated Systems, San Diego, CA, 2005.
[11] M. Ahmadian and J.C. Poynor, *An evaluation of magneto rheological dampers for controlling gun recoil dynamics*, Shock Vib., 8 (2001), pp. 147–155.
[12] M. Ahmadian, R. Appleton, and J.A. Norris, *An analytical study of fire out of battery using magneto rheological dampers*, Shock Vib., 9 (2002), pp. 129–142.
[13] M. Ahmadian, R.J. Appleton, and J.A. Norris, *Designing Magneto-Rheological Dampers in a Fire Out-of-Battery Recoil System*, 11th Symposium on Electromagnetic Launch (EML) Technology, USA, 2003.
[14] H. Hu, J. Wang, J. Wang, S. Qian, and Y. Li, *Investigation on Modeling and Controability of a Magnetorheological Gun Recoil Damper*, Proceedings of the 2nd International Conference on Smart Materials and Nanotechnology in Engineering, Weihai, China, 2009.
[15] H. Hu, J. Wang, S. Qian, Y. Li, and X. Jiang, *Investigation on Controllability of a Magnetorheological Gun Recoil Damper*, Proceedings of the International Conference on Information and Automation (ICIA), Piscataway, NJ, 2009.
[16] Z. Lijie, M. Fugui, and W. Jiong, *Study of Control System of Magnetorheological Dampers Under Impact Load*, Proceedings of the Second International Conference on Intelligent Computation Technology and Automation (ICICTA), Piscataway, NJ, 2009.
[17] E.L. Kathe, *Recoil considerations for railguns*, IEEE Transactions on Magnetics, 37(1) (2001), pp. 425–430.
[18] D. Karnopp, M.J. Crosby, and R.A. Harwood, *Vibration control using semi-active force generators*, J Eng Ind Trans ASME, 96 (1974), pp. 619–626.
[19] J. Aardema, *Failure analysis of the lower rear ball joint on the high-mobility multipurpose wheeled vehicle (HMMWV)*, Technical Report, Army Tank-Automotive Command, Warren MI, 1988.
[20] A. Berghuvud and A. Stensson, *Consequences of nonlinear characteristics of a secondary suspension in a three-piece freight car bogie*, Veh. Syst. Dyn., 36 (2001), pp. 37–55.
[21] A. Bedford and W. Fowler, *Engineering Mechanics: Statics*, Pearson Prentice Hall, Upper Saddle River, NJ, 2008.
[22] R.M. Bhatnagar, *Recoil motion theorem*, Proc. Inst. Mech. Eng., Part K: J. Multi-body Dyn., 219 (2005), pp. 173–176.
[23] Physics Central, *Answering the call for extreme tires*. (2011). Available at http://www.physicscentral.com/explore/action/extremetires1.cfm.

Nomenclature

Symbol	Definition
F_r	recoil force
m_r	recoil mass
m_{tr}	rear unsprung mass
m_{tf}	front unsprung mass
m_c	mortar–chassis mass
m_{ch}	chassis mass
m_{mor}	mortar mass
I_c	mortar–chassis mass moment of inertia
I_{ch}	chassis mass moment of inertia
I_{mor}	mortar mass moment of inertia
k_r	recoil stiffness
k_{cr}	rear suspension stiffness

k_{cf} front suspension stiffness
k_{tr} rear tyre stiffness
k_{tf} front tyre stiffness
k_{hr} rear horizontal stiffness of chassis
k_{hf} front horizontal stiffness of chassis
c_r recoil damping coefficient
c_{cr} rear suspension damping coefficient (stock passive suspension)
c_{cf} front suspension damping coefficient (stock passive suspension)
c_{tr} rear tyre damping coefficient
c_{tf} front tyre damping coefficient
c_{hr} rear horizontal damping coefficient of chassis
c_{hf} front horizontal damping coefficient of chassis
L vehicle wheelbase
a distance from mortar–chassis centre of gravity to front of the car
b distance from mortar–chassis centre of gravity to rear of the car
c horizontal distance from mortar–chassis centre of gravity to mortar connection point to chassis
f distance from mortar centre of gravity to its connection point to chassis
e distance from chassis centre of gravity to rear of the car
d distance from chassis centre of gravity to front of the car
h horizontal distance from chassis centre of gravity to mortar connection point to chassis
α mortar elevation angle from horizon
h_c vertical distance from mortar–chassis centre of gravity to mortar connection point to chassis
h_r vertical distance from mortar–chassis centre of gravity to rear suspension
h_f vertical distance from mortar–chassis centre of gravity to front suspension
h_{cf} vertical distance from chassis centre of gravity to front suspension
h_{cr} vertical distance from chassis centre of gravity to rear suspension
h_{ch} vertical distance from chassis centre of gravity to mortar connection point to chassis
y_{cg} vertical distance from chassis centre of gravity to that of mortar–chassis system